ELSEVIER

Carbohydrate Polymers 49 (2002) 121–129

Carbohydrate Polymers

www.elsevier.com/locate/carbpol

Cell wall changes in ripening kiwifruit: ^{13}C solid state NMR characterisation of relatively rigid cell wall polymers

R.H. Newman[a], R.J. Redgwell[b,*]

[a]*Industrial Research Limited, P.O. Box 31-310, Lower Hutt, New Zealand*
[b]*Horticultural and Food Research Institute of New Zealand Ltd, Private Bag 92169, Auckland, New Zealand*

Received 10 January 2001; revised 12 July 2001; accepted 16 July 2001

Abstract

Cell wall material was isolated from the outer pericarp of kiwifruit at harvest and at several ripening stages following a postharvest ethylene treatment. Solid state ^{13}C NMR spectra showed no evidence for changes in the nature of the cellulose crystallites or the polysaccharides adhering to crystallite surfaces even in cell wall material isolated from fruits in which cell wall dissolution was extreme. Nuclear spin relaxation experiments showed that pectin retained in the cell wall became 'softened' in the early stages of ripening, prior to solubilisation later in ripening. Chemical data showed that this 'softening' of pectin was not accompanied by any marked change in its chemical composition. Fruit firmness was directly proportional to the amount of non-cellulosic matter that remained sufficiently rigid to respond to the cross-polarisation NMR pulse sequence. The results support the idea that pectin solubilisation in ripening fruit may in part be a consequence of cell wall swelling rather than a direct cause of it.

Keywords: Kiwifruit; NMR spectroscopy; Cellulose; Pectin; Ripening

1. Introduction

It is widely accepted that the softening of fruits which accompanies ripening is largely caused by changes in the physicochemical properties of the cell wall (John & Dey, 1986). In kiwifruit and many other fruit species the softening process is accompanied by a marked swelling of the cell wall, which shows a strong correlation with solubilisation of the pectic polysaccharides (Redgwell, MacRae, Hallet, Fischer, Perry & Harker, 1997). It has been postulated that swelling may in part result from water moving into the voids left by the solubilised pectin but the exact mechanism for solubilisation is not known. The high molecular weight of solubilised pectin from several different fruits suggest that solubilisation is caused by processes other than enzymatic depolymerisation of the cell wall pectin. Such processes may involve disruption of interactions between adjacent cellulose microfibrils, or between those microfibrils and the matrix polysaccharides.

Little effort has been concentrated on the question of changes to such interactions during ripening because the available chemical procedures have been inadequate. Solid state ^{13}C NMR has recently emerged as a means of monitoring the rigidity or mobility in plant cell walls (Jarvis, 1990; Jarvis & Apperley, 1990) and has been used to characterise changes in molecular motion in apple cell walls (Irwin, Gerasimowicz, Pfeffer, & Fishman, 1985; Irwin, Pfeffer, Gerasimowicz, Pressey & Sams, 1984; Irwin, Sevilla, Chamulitrat, Hoffman & Klein, 1992 and tomato cell walls (Fenwick, Jarvis, Apperly, Seymour & Bird, 1996) during ripening. Newman, Davies and Harris (1996) and Newman, Ha and Melton (1994) have shown that solid state NMR is sufficiently sensitive to provide information about crystalline forms of cellulose and to test for the presence of polysaccharides adhering to cellulose microfibrils.

In this paper we describe the use of solid state ^{13}C NMR for characterisation of the relatively rigid polymers in kiwifruit. We use the term 'relatively rigid' for any polymers which respond to the cross-polarisation (CP) NMR pulse sequence, combined with magic angle spinning (MAS). The relatively rigid polymers include crystalline cellulose, any adhering polysaccharides, and the more rigid pectin-rich domains. The term 'relatively mobile' is used for any polymers which respond to the single-pulse excitation (SPE) pulse sequence when combined with MAS. SPE NMR is commonly used for study of liquid samples, and the

* Corresponding author. Present address: Nestlé Research Center, Nestec Ltd., Vers-Chez-Les- Blanc, P.O. Box 44, CH-1000 Lausanne 26, Switzerland. Tel.: +41-21-785-8681; fax: +41-21-785-8554.

E-mail address: robert.redgwell@rdls.nestle.com (R.J. Redgwell).

0144-8617/02/$ - see front matter
PII: S0144-8617(01)00323-X

Table 1
CWM extraction data for kiwifruit at 5 ripening stages

Stage	Firmness (kg)	CWM[a] (g)	PAW-soluble polyuronide[a] (mg)	Swelling (mm)
Harvest	8.3	1.3	5	2
1 day	6.1	1.2	25	4
2 day	4.1	1.0	114	7
4 day	2.1	1.0	172	9
6 day	< 0.1	0.7	324	35

[a] isolated from 120 g fresh weight outer pericarp

SPE/MAS NMR will elicit responses from galactans, arabinans and some of the relatively mobile pectins in plant cell walls (Foster, Ablett, McCann & Gidley, 1996; Ha, Evans, Jarvis, Apperley & Kenwright, 1996).

2. Experimental

2.1. Isolation of Cell Wall Materials (CWM)

Samples of kiwifruit (*Actinidia deliciosa*) were taken at harvest and 1, 2, 4, and 6 days after treatment with ethylene (Redgwell, Melton & Brasch, 1992). Tissue firmness (Table 1) was measured at each stage of ripening with an effigi penetrometer (Effigi, Alfonsine, Italy).

CWM was isolated as described in Redgwell et al. (1992). At each sampling time duplicate fruit samples (10 fruit per sample) were taken. Fruits were peeled and the outer pericarp cut into 2 cm^3 pieces, frozen in liquid nitrogen and cryomilled to a fine powder. The powder (120 g) was suspended in 240 ml of PAW (phenol:acetic acid:water. 2:1:1 w/v/v) and homogenised with a Polytron to a fine slurry. The homogenate was centrifuged (4000 g, 10 min) and the residue resuspended in water and centrifuged. The PAW-insoluble residue, henceforth referred to as CWM, was suspended in 90% DMSO and stirred overnight to solubilise starch. The CWM was recovered after centrifugation, washed several times with water and then suspended in 80% ethanol pending examination by solid state NMR. A portion of CWM was freeze-dried immediately after the water wash for chemical analysis and swelling measurements. Swelling of the CWM was determined by suspending 10 mg of the dried CWM in 3 ml water and measuring the thickness of the sedimented layer (Redgwell et al., 1997).

The PAW-soluble fraction and the water wash were combined and dialysed. The contents of the dialysis tubing were then centrifuged and the supernatant freeze-dried to give the PAW-soluble fraction.

The monosaccharide composition of the CWM (Table 2) was determined by capillary GC of the alditol acetates following TFA hydrolysis (Albersheim, Nevins, English & Karr, 1967). The uronic acid content was measured by the method of Blumenkrantz and Asboe-Hansen (1973).

Table 2
Monosaccharide composition of non-cellulosic polysaccharides in CWM isolated from kiwifruit at 5 stages of ripening

Stage	Composition (μg/mg CWM)						
	Rha	Ara	Xyl	Man	Gal	Glc[b]	Uronic acid
Harvest	9.6	11.1	29.2	5.9	98.9	58.9	300
1 day	10.8	12.3	30.6	4.8	99.4	19.9	300
2 day	11.0	11.9	33.9	6.5	105.3	27.0	259
4 day	10.8	11.5	39.5	7.7	78.9	19.1	257
6 day	3.3	4.6	50.5	11.6	29.2	20.1	153

[b] The increased amount of glucose in the CWM of the harvest sample is caused by residual starch which is very high in unripe kiwifruit.

2.2. NMR Spectroscopy

A portion of each suspension was filtered using Whatman GFA glass fibre filter paper. The CWM was air dried until it attained a solid content of $50 \pm 5\%$ by weight (estimated by oven drying a subsample), packed in a 7 mm diameter cylindrical silicon nitride rotor, and retained with vespel end caps. Each rotor was spun at 3.5 ± 0.5 kHz in a Doty Scientific magic-angle spinning probe for ^{13}C CP/MAS NMR spectroscopy at 50.3 MHz on a Varian Inova-200 spectrometer.

Resolution-enhanced NMR spectra were generated from data averaged over periods of 52 h (CWM at harvest) or 30 h (6 days after ethylene treatment). NMR spectra of the other three samples were not averaged over sufficiently long periods to attain the signal-to-noise ratios needed for successful resolution enhancement. Each 6 μs proton preparation pulse was followed by a 1 ms cross polarisation contact time, 50 ms of data acquisition and a recovery delay of 1.5 s before the sequence was repeated. The decoupler field strength was increased to provide a proton rotating frame precession frequency of >50 kHz for data acquisition. Resolution enhancement was achieved by convoluting NMR free induction decays with a function of the form (Newman et al., 1994)

$$f(t) = \exp\{(t/T_x)^2/2minus; (t/T_Y)^3/3\} \quad (1)$$

Values of $T_x = 6$ ms and $T_Y = 9$ ms were used for similar studies of apple cell walls (Newman et al., 1994).

Proton spin relaxation edited (PSRE) NMR subspectra

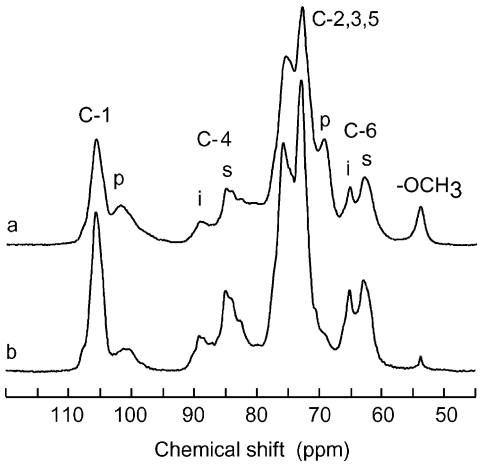

Fig. 1. CP/MAS NMR spectra of kiwifruit cell walls isolated (a) at harvest, (b) 6 days after treatment with ethylene, plotted without resolution enhancement. Carbon numbers refer to cellulose with labels i and s used to distinguish signals assigned to crystallite interiors and surfaces. Signals assigned primarily to pectins are labelled *p*.

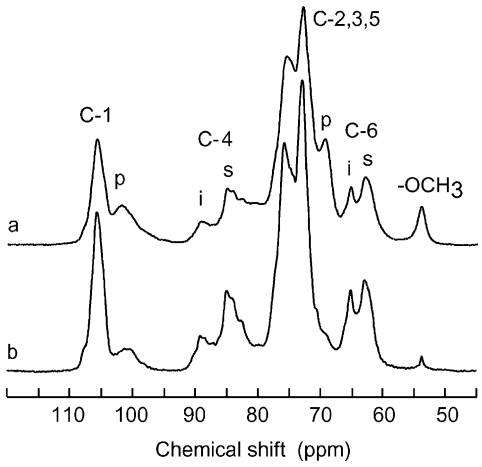

Fig. 2. CP/MAS NMR spectra of (a) microcrystalline cellulose I, (b) a portion of the same sample transformed to cellulose II.

were generated by combining spectra Labelled S and S′, where S represents the spectrum obtained by the normal cross-polarisation pulse sequence, as used for resolution enhancement, and S′ represents a 'delayed contact' spectrum obtained by inserting a proton magnetisation spin-locking pulse of duration 4 ms between the proton preparation pulse and the CP contact time. Each spectrum (S or S′) was averaged over a period of at least 4 h.

The principles behind PSRE NMR have been described elsewhere (Newman et al., 1994; Newman, 1992; Newman & Hemmingson, 1990). In the present context, signals at 89 and 69 ppm were taken as representative of the most rigid and less rigid polymers, respectively. Relative peak heights at these two chemical shifts were used to estimate values of $T_{1\rho}$ (H) for the two categories of polymers, and these values of $T_{1\rho}$ (H) were used to calculate coefficients for two subspectra (labelled A and B) corresponding to the two categories of polymers.

Proton spin–spin relaxation time constants were measured by switching off the proton- frequency transmitter for a delay t between the 90° proton preparation pulse and commencement of the cross-polarisation contact time (Alla & Lippmaa, 1976). Signal heights $h(t)$ were interpreted in terms of decay curves of the form:

$$h(t) = h(0)\exp\{minus; t^2/(2T_2^2)\} \quad (2)$$

A sample of commercial microcrystalline cellulose (Avicel) was purchased from Merck Chemical company. The microcrystalline cellulose was moistened to 41% water and a ^{13}C NMR was obtained as for kiwifruit CWM, except that the recovery delay was extended to 4 s and data averaging was limited to 44 h. A portion of the microcrystalline cellulose was transformed to the cellulose II crystalline form by immersion overnight in 16% (w/w) NaOH, followed by thorough washing with distilled water. A ^{13}C NMR spectrum was obtained under conditions similar to those used for the microcrystalline cellulose I.

Chemical shifts were referenced relative to TMS, using the methyl signal of hexamethylbenzene as a secondary reference with a chemical shift of 17.4 ppm.

3. Results and discussion

3.1. Fruit ripening

Between harvest and 6 days after ethylene treatment, fruits softened from 8.3 to less than 0.1 kgf (Table 1). Two days after ethylene treatment there was a detectable decrease in the polyuronide content of the CWM but the biggest loss of polyuronide occurred between 4 and 6 days after harvest. A 4.5 fold increase in wall swelling occurred between 4 and 6 days after ethylene treatment, in synchrony with pectin solubilisation (Table 1). The CWM at each ripening stage showed little change in monosaccharide composition between harvest and 4 days after ethylene treatment, with the exception of a 20% decrease in the galactose content after 4 days (Table 2). There was a dramatic loss in all pectin-associated monosaccharides (rhamnose, arabinose, galactose and uronic acid) 6 days after ethylene treatment.

3.2. Overview of signal assignments

The dominant signals in the spectra of kiwifruit CWM (Fig. 1a and b) resemble those in the spectrum of microcrystalline cellulose I (Fig. 2a) except for differences in the relative strength of signals assigned to cellulose chains in crystallite interiors and on crystallite surfaces labelled i and s respectively. The dominant signals do not resemble those in the spectrum of cellulose II (Fig. 2b), although possible matches amongst minor signals are discussed in more detail below.

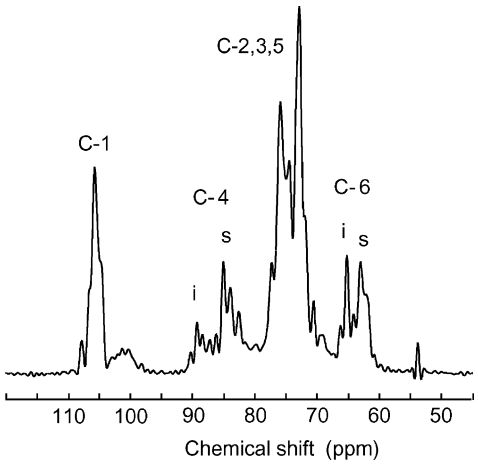

Fig. 3. Resolution-enhanced CP/MAS NMR spectrum of kiwifruit cell walls isolated 6 days after treatment with ethylene.

The spectra of CWM also showed signals assigned to non-cellulosic polymers, stronger in Fig.1a than in Fig. 1b. The loss of signal strength is attributed to a combination of loss of polyuronide in the PAW-soluble fraction (Table 1) and loss of rigidity in the remaining non-cellulosic material. Loss of rigidity affects the efficiency of the CP NMR process, which is designed to elicit a response from a rigid solid sample.

Signals at 101, 79, and 69 ppm are assigned to C-1, C-4 and C-2 galacturonic acid units in pectins, and a signal at 54 ppm is assigned to $-OCH_3$ carbon in methyl esterified pectins (Colquhoun, de Ruiter, Schols & Voragen, 1990). Solution NMR spectra of pectins show signals at 71 and 72 ppm, assigned to C-3 and C-5 of galacturonic acid units. The corresponding signals could not be resolved from overlapping cellulose signals in Fig. 1a and b. The spectra of kiwifruit CWM showed signals outside the chemical shift range displayed in Fig. 1, between 170 and

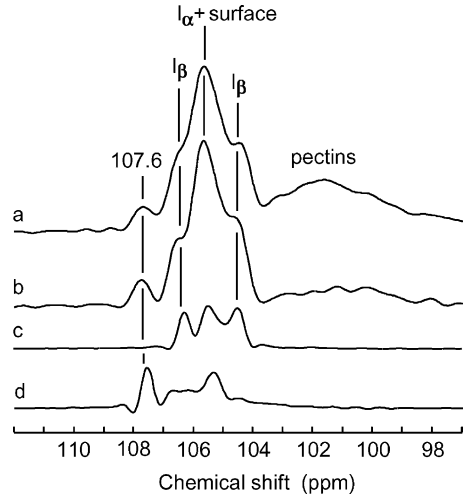

Fig. 4. Resolution-enhanced C-1 region of CP/MAS NMR spectra of (a) kiwifruit cell walls isolated at harvest, (b) cell walls isolated 6 days after treatment with ethylene (c) microcrystalline cellulose I, (d) cellulose II.

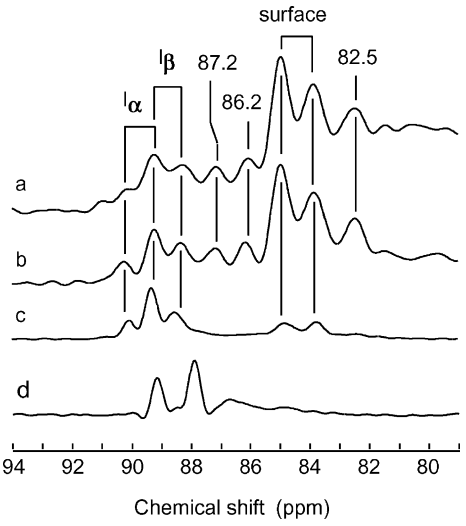

Fig. 5. Resolution-enhanced C-4 region of CP/MAS NMR spectra of (a) kiwifruit cell walls isolated at harvest, (b) cell walls isolated 6 days after treatment with ethylene (c) microcrystalline cellulose I, (d) cellulose II.

175 ppm. These signals were assigned to the carbonyl carbon (C-6) of galacturonic acid units. Relatively weak responses were attributed to the lack of a directly-bonded H atom on C-6, and the consequent dependence on relatively slow cross polarisation processes involving more distant protons.

3.3. Celluloses I_α and I_β

Resolution-enhancement (Fig. 3) splits peaks assigned to cellulose into components assigned to two crystalline forms, designated cellulose I_α and I_β (Atalla & Vanderhart, 1984). The component signals are shown more clearly in expanded plots of three chemical shift ranges (Figs. 4–6). Signal assignments shown above the plots are based on those published by (Atalla and Vanderhart (1984) and VanderHart and Atalla (1984)). The C-1 region (Fig. 4) is not particularly

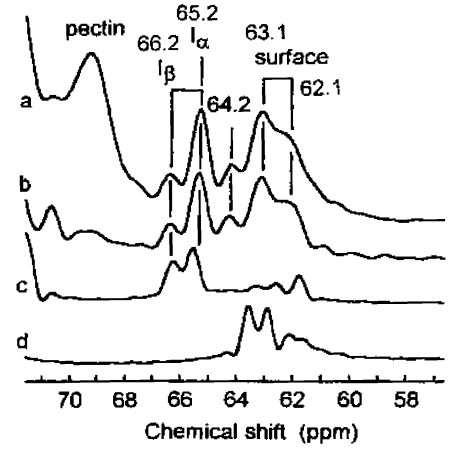

Fig. 6. Resolution-enhanced C-6 region of CP/MAS NMR spectra of (a) kiwifruit cell walls isolated at harvest, (b) cell walls isolated 6 days after treatment with ethylene I, (c) microcrystalline cellulose I, (d) cellulose II.

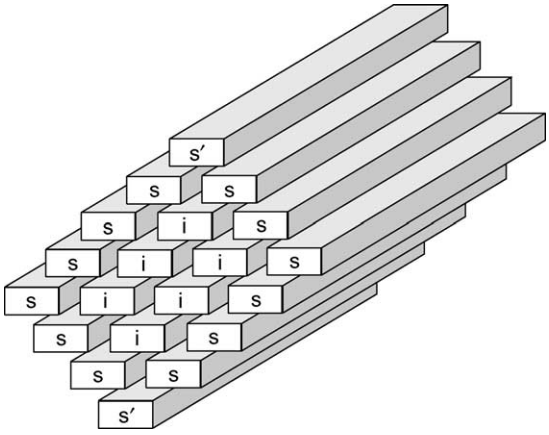

Fig. 7. Representation of a section through a cellulose crystallite. Each rod represents a cellulose chain, and hydrogen bonds are confined to the horizontal planes, Labels i and s refer to interior and surface chains, respectively, and s′ refer to surface chains that lack hydrogen bonds to any other chains.

informative because a signal assigned to crystallite-surface chains (discussed in Section 3.4) is superimposed on a signal assigned to cellulose I_α so it is not possible to estimate the content of cellulose I_α. Shoulders at 104.5 and 106.3 ppm in Figs 4a and 4b indicate that cellulose I_β is present in the cell walls. Relative strengths of C-4 signals at 88.4 and 90.2 ppm in Fig. 5a and b suggest cellulose I_α and I_β might be present in similar proportions but it is not possible to estimate the relative proportions because of overlap from neighbouring signals. In the C-6 region (Fig. 6) the strength of a signal at 65.2 ppm, relative to a signal at 66.3 ppm is attributed to overlapping contributions from both I_α and I_β crystalline forms at 65.2 ppm.

Whatever the relative proportions of both the I_α and I_β crystalline forms it seems clear that they are not affected by ripening processes.

3.4. Cellulose crystallite surfaces

The word crystallite is used to indicate a crystalline domain within a microfibril. The crystallites might be separated by disordered regions (Dolmetsch & Dolmetsch, 1968) or by strain distorted 'tilt and twist' regions (Rowland & Howley, 1988). Each crystalline domain is envisaged as extending across the entire width of the microfibril, so a cross section (Fig. 7) shows an ordered array of chains. Some of the chains (labelled i in Fig. 7) are enclosed within the crystallite interior. Each of these chains is linked by hydrogen bonding to two adjacent chains (Gardner & Blackwell, 1974). Hydrogen bonding is confined to the horizontal planes in Fig. 7. Some of the chains (labelled s in Fig. 7) are exposed on a crystallite surface. Most of these chains are linked by hydrogen bonding to just one adjacent chain. Two chains (labelled s′ in Fig. 7) are not linked by hydrogen bonding to any other chains.

The chains labelled s′ were omitted from an earlier illustration (Newman et al., 1994) because the lack of hydrogen bonds seemed to make cohesion unlikely. Recent computations have indicated that van der Waals forces, rather than hydrogen bonds, provide the dominant cohesive forces in a cellulose crystallite (Cousins & Brown, 1995), so the possibility of finding chains at the positions labelled s′ must be considered. Signals from these chains are expected to be relatively weak, and will be discussed under the heading 'Minor Components Associated with cellulose'.

The repeating unit in a cellulose chain is cellobiose, not glucose, so the glucosyl units in a crystallite surface are located in two distinct environments. In one environment the $-CH_2OH$ group points towards the crystallite interior, in the other it is exposed on the surface. The chemical shift displacement between signals labelled i and s is attributed to changes in torsional angles about β-(1 → 4)-glycosidic linkages, caused by hydration of exposed $-CH_2OH$ groups and consequent disruption of the pattern of intramolecular hydrogen bonding described by Gardner and Blackwell (1974). Signals at 83.9 and 85 ppm in Fig. 5a and b are assigned to C-4 in chains exposed on crystallite surfaces (Newman et al., 1996; Newman et al., 1994; Newman & Hemmingson, 1995). The C-4 chemical shift is particularly sensitive to changes in torsional angles about the β-(1 → 4)-glycosidic linkage (Horii, Hirai, & Kitamaru, 1984, so the displacement of about 5 ppm from signals assigned to crystallite interior is consistent with the explanation discussed above. The relative strength of crystallite surface signals indicates that chains exposed on surfaces outnumber chains enclosed within the interior of a typical crystallite as in the representation (Fig. 7).

Signals at 62.1 and 63.1 ppm in Fig. 6a and b are assigned to C-6 in chains exposed on crystallite surfaces, i.e. those labelled s in Fig. 7. The chemical shifts do not quite match values of 61.7 and 62.5 ppm for the corresponding signals in the spectrum of microcrystalline cellulose I (Fig. 6c).

3.5. Minor components associated with cellulose

Figs. 4–6 show minor signals at 107.6, 87.2, 86.2, 82.5 and 64.2 ppm in the spectra of the kiwifruit cell walls. None of these minor signals appear in the corresponding plot expansions from the spectrum of microcrystalline cellulose I (Figs. 4–6c). Whatever the assignment of these minor signals, relative strengths in Figs. 4–6 indicate no change related to ripening. The signals are however, of interest in that the patterns of relative signal strengths indicate differences in molecular organisation between cell walls of kiwifruit and those of apples (Newman et al., 1994) or *Arabidopsis thaliana* (Newman et al., 1996).

The minor signals can be seen as shoulders or partly resolved peaks in spectra plotted without resolution (Fig. 1), so they cannot be dismissed as artifacts introduced by resolution-enhancement processing. The relatively sharp lineshapes seem consistent with well-ordered material. Values of $T_2(H) = 9 \pm 1$ μs were estimated for all five

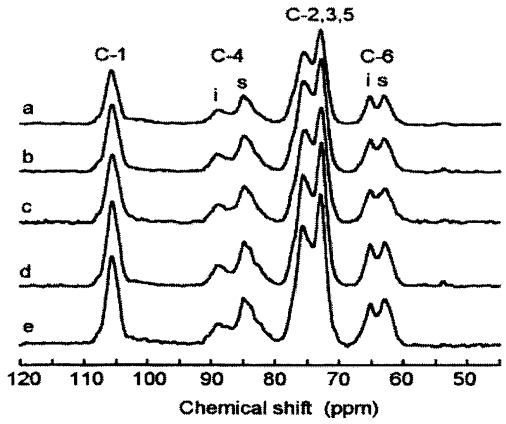

Fig. 8. Subspectra labelled A, separated from the CP/MAS NMR spectra of kiwifruit cell walls isolated (a) at harvest, (b) 1 day, (c) 2 days, (d) 4 days, (e) 6 days after treatment with ethylene. Carbon numbers refer to cellulose. All subspectra plotted at the same signal amplification.

minor signals in experiments on the sample of cell walls sampled 6 days after exposure to ethylene. These results cannot be distinguished from values of $T_2(H) = 9.4 \pm 0.5$, 8.9 ± 0.3 and 9.0 ± 0.3 μs for crystalline cellulose I obtained through measurements at 89.4, 85.0, and 65.2 ppm respectively. The latter values are relatively precise because they are based on stronger signals. Similarities between values of T_2(H) for the unidentified components and values for crystalline cellulose are attributed to physical association, allowing proton spin diffusion to mix spin information between the unidentified components and underlying cellulose crystallites.

Longer values of T_2(H) are expected for non-crystalline polymers and in the present case a value of $T_2 = 23$ μs was measured for the signal at 69 ppm, assigned to pectins. The distinction between T_2(H) for crystalline and non-crystalline environments is important because kiwifruit cell walls contain arabinosyl units. The relevant C-1 chemical shifts are in the range 107.6 to 108.7 ppm (Capek, Toman, Kardosova & Rosik, 1983), but the arabinosyl units are expected to occur in non-crystalline environments. The arabinosyl units might not even be sufficiently rigid to contribute to CP/MAS NMR spectra. (Foster et al. (1996)) found that the arabinans of onion cell walls responded to SPE/MAS NMR, so that the polymers must be relatively mobile. The relatively short value of T_2 (H) measured for the signal at 107.6 ppm in Fig. 4b seems to preclude assignment to arabinosyl units.

The signal at 107.6 ppm coincides with a signal in the spectrum of cellulose II (Fig. 4d). Signals from the other 5 carbon atoms in each cellulose II glycosyl unit (Fig. 2b) are found at chemical shifts overlapping cellulose I signals (Fig. 2a) so supporting evidence for cellulose II is not readily obtained. Plot expansions of the chemical-shift ranges associated with C-4 and C-6 of cellulose (Figs. 5 and 6) show no signal that is unique to cellulose II. The signal at 107.6 ppm provides evidence for cellulose chains in a molecular conformation similar to that of cellulose II, but does not necessarily provide evidence for molecular organisation in the cellulose II crystalline form. The observation could be consistent with the chains labelled s′ in Fig. 7, adopting a conformation similar to that of cellulose II while adhering to chains in the cellulose I conformation.

Spectra of kiwifruit cell walls (Fig. 5a and b) both show a signal at 82.5 ppm, absent from spectra of microcrystalline cellulose I and II (Fig. 5c and d) and from spectra of apple and *Arabidopsis thaliana* cell walls (Newman et al., 1996, 1994). The chemical shift is consistent with the value of 83 ppm reported for C-4 xylans adhering to cellulose crystallite surfaces (Mitikka, Teeaar, Tenkanen, Laine & Vuorinen, 1995). This is very different from a chemical shift of 77 ppm reported for C-4 of xylans in solution. The difference has been attributed to a change in the conformation of xylan chains, from a disordered conformation in solution to a conformation with a two-fold screw axis in xylan chains adhering to cellulose chains (Mitikka et al., 1995). Kiwifruit cell walls contain xylans (Redgwell, Melton & Brasch, 1988). But it is doubtful whether the reported levels would be adequate to account for the strength of signal at 82.5 ppm in Fig. 5a and b. (Redgwell et al. (1988)) prepared polysaccharide fractions by stepwise extraction of cell wall material sampled from the outer pericarp of kiwifruit, then determined linkage patterns by methylation analysis in order to distinguish between xylans (in which the xylosyl units are connected by β 1–4 linkages) and xyloglucans (in which the xylosyl units are substituted to a glucan backbone). They found evidence for xylans in several fractions, the total amount accounting for about 1.5% of all residues in the cell wall. An insoluble cellulosic residue accounted for about 43% of the cell wall material. The xylan/cellulose ratio is about half of that required to account for the strength of the signal at 82.5 ppm.

The major hemicellulose of kiwifruit is a xyloglucan (Redgwell et al., 1988). Xyloglucans have been shown to bind to cellulose fibrils in-vitro and in-vivo (Hayashi, Marsden & Delmer, 1987) but little is known about the NMR chemical shifts for the bound material. Whitney, Brigham, Darke, Reid and Gidley (1995) published a resolution-enhanced CP/MAS NMR spectrum of a cellulose–xyloglucan complex, but the signal-to-noise ratio was not adequate for the xyloglucan C-4 signals to emerge. Their spectrum showed a signal at 99.5 ppm, assigned to xylosyl C-1 in cellulose-associated segments of the xyloglucan. Fig. 4 shows signal strength at that chemical shift, but only as a component of an unresolved band. Chemical shifts for xyloglucan in solution include a value of 89.1 ppm for C-4 in glycosyl units linked to xylosyl units through C-6 (York, Harvey, Guillen, Albersheim & Darvill, 1993), but this value is expected to increase as the molecular conformation changes to adopt the two-fold screw axis required for compatibility with cellulose (Levy, York, Stuike-Prill, Meyer & Staehlin, 1991). Chemical shifts for the xylosyl units seem less likely to be affected by the interaction with

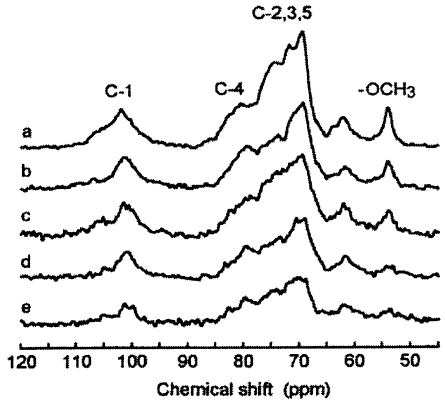

Fig. 9. Subspectra labelled B, separated from the CP/MAS NMR spectra of kiwifruit cell walls isolated (a) at harvest, (b) 1 day, (c) 2 days, (d) 4 days, (e) 6 days after treatment with ethylene. Carbon numbers refer to galacturonic acid units. Signal amplification as in Fig. 8.

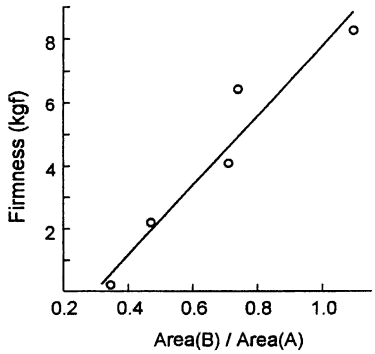

Fig. 10. Relationship between fruit firmness and the relative signal areas of subspectra A and B. The straight line represents the linear least-squares best fit.

cellulose. Values of 100.0 (C-1), 72.3 (C-2), 73.8 (C-3), 70.3 (C-4) and 62.3 ppm (C-5) have been reported for a xyloglucan in solution (York et al., 1993). None of these values approach the value of 82.5 ppm for the unidentified signal.

If the signal at 82.5 ppm is associated with a xyloglucan–cellulose complex, then it raises the question of why the signal is present in NMR spectra of kiwifruit cell walls but not in spectra of apple cell walls or *Arabidopsis thaliana* leaf cell walls (Newman et al., 1996, 1994). Xyloglucan is a major polysaccharide in all three cases but it would be difficult to explain why it would form a complex with cellulose in one species but not the others.

3.6. Edited NMR subspectra

Proton spin relaxation editing was used to separate each spectrum into two component subspectra, labelled A (Fig. 8) and B (Fig. 9). The mean value of $T_{1\rho}(B)/T_{1\rho}(A) = 0.37$ (standard deviation 0.03) confirms a clear distinction between the more rigid (long $T_{1\rho}$) and less rigid (short $T_{1\rho}$) domains for all five samples. Signals in subspectrum A are assigned to crystalline cellulose and associated polysaccharides. Signals in subspectra B are assigned to pectins and disordered polysaccharides in environments less rigid than cellulose, but sufficiently rigid for the material to respond to the cross polarisation NMR sequence. Each of the two categories will be discussed in turn.

3.7. Subspectra labelled A

Comparisons within Fig. 8 show no evidence for changes with time in the nature of the cellulose and associated polysaccharides, although the amount increases when expressed as a fraction of total NMR-responsive material.

Separation of NMR subspectra led to the estimation of cellulose crystallite cross-sectional dimensions for cell walls from apples and *Arabidopsis thaliana* leaves (Newman et al., 1996, 1994). Interferences from minor signals discouraged any such estimation in the case of kiwifruit CWM. Signals at 86.2 and 87.2 ppm blurred the distinction between C-4 signals assigned to crystallite interior and surface chains, and a signal at 82.5 ppm was not fully resolved from the signals assigned to surface chains. Whatever the cellulose crystallite cross-sectional dimensions might be, the unchanging band profiles in Fig. 8 suggest that they are not affected by ripening processes.

3.8. Subspectra labelled B

All five subspectra in Fig. 9 are dominated by a signal at 69 ppm, assigned to C-2 of galacturonic acid units, and show a signal at 62 ppm, assigned to C-5 or C-6 of pentosyl or hexosyl neutral carbohydrate units e.g. C-5 of xylosyl units in xyloglucans or xylans, or C-6 of mannosyl units in mannans. None of the subspectra show a signal at 105 ppm, i.e the chemical shift of C-1 in non-crystalline cellulose (Newman et al., 1995; Newman, Hemmingson & Suckling, 1993). The C-1 signal provides a useful test for the presence of non-crystalline cellulose, since signals from the other 5 carbon atoms occur at chemical shifts which coincide with signals from non-cellulosic matter.

Comparisons within Fig. 9 show that the nature of the non-cellulosic material changes during ripening, in that the relative strength of the methoxyl signal diminishes.

It must be stressed that the loss of signal strength from the sub-spectrum B is not necessarily the result of solubilisation and removal from the cell wall, but can be explained in terms of softening of polymeric structures, i.e. change from a relatively rigid (solid-like) state to a more mobile (liquid like) state which does not respond to the cross polarisation pulse sequence. This point is supported by compositional data for the CWM in Tables 1 and 2 which show little change in the content of uronic acid over the first 4 days and then a sudden decline between 4 and 6 days. We attribute the steady loss of NMR signal strength over the first 4 days of ripening to softening of pectic matter retained in the cell wall. In other words the NMR experiments have revealed an

aspect of the ripening process that could not have been investigated by chemical analysis.

3.9. Correlations with firmness and swelling

Fig. 10 shows a correlation between the original amount of NMR-responsive non-cellulosic material and the firmness of the fruit. The area of sub-spectrum B includes signals outside the chemical shift range shown in Fig. 9, e.g. signals from C-1 of galacturonic acids and methoxyl esters in the range 170 to 175 ppm. A linear-least squares fit, represented by a line drawn in Fig. 10, indicates a correlation coefficient $R = 0.966$ for the relationship.

The 'polymer-softening' phenomenon associated with the early stages of ripening is accompanied by a four fold swelling in the CWM, 4 days after ethylene treatment. However, there is only a very small loss in the uronic acid content and no loss in the rhamnose content of the CWM (Table 2). This suggests that whatever chemical changes bring about this softening, it does not involve solubilisation of the rhamnogalacturonan regions of the pectic backbone. Nevertheless, the increase in the polyuronide content of the PAW-soluble fraction 1 and 2 days after ethylene treatment (Table 1) shows that some pectin solubilisation is taking place, perhaps favouring the more homogalacturonan structures that are believed to make up the middle lamella. Following loosening of the middle lamella, chemical changes later in ripening may lead to lower degrees of cross-linking of the non-cellulosic polysaccharides of the primary wall allowing the wall to swell. The molecules that become less cross-linked and more mobile do not respond to the cross-polarisation NMR pulse sequence. At this point pectic polysaccharides within the primary wall become accessible to hydration and solubilisation, which in turn leads to further swelling and more solubilisation. Since pectic polysaccharides of the primary cell wall contain highly branched polymers (Redgwell et al., 1992) their solubilisation leads to a marked decrease in the rhamnose, galactose and arabinose content of the CWM 6 days after ethylene treatment (Table 2). At the present time we do not know the nature of the cross-linking between non-cellulosic polymers or the agents that mediate their hydrolysis. Any polysaccharide bridges between crystallites and the surrounding matrix might be too flexible to contribute to the CP/MAS NMR spectrum. However, indirect evidence for their existence is provided by the fact that Na_2CO_3 solutions can cause a marked swelling of kiwifruit CWM while solubilising a major portion of the cell wall pectin without detectable depolymerisation (Redgwell et al., 1997).

4. Conclusions

Ripening processes in kiwifruit do not affect the nature of cellulose crystallites or the nature of polysaccharides adhering to surfaces of cellulose crystallites. Ripening processes result in loss of rigidity in the pectic domains, initially through softening of polymer molecules until they lack the rigidity required for an efficient response to the cross polarisation pulse sequence, later through solubilisation of pectic matter and removal from the cell wall. The firmness of the fruit is proportional to the residual amount of rigid non-cellulosic matter in the cell walls.

Acknowledgements

The New Zealand Foundation for Research Science and Technology is thanked for funding under contract CO6242.

References

Albersheim, P., Nevins, D. J., English, P. D., & Karr, A. (1967). A method for the analysis of sugars in plant cell wall polysaccharides by gas-liquid chromatography. *Carbohydrate Research*, *5*, 340–345.

Alla, M., & Lippmaa, E. (1976). High resolution broadline ^{13}C NMR and relaxation in solid norbornadiene. *Chemical Physical Letters*, *37*, 260–264.

Atalla, R. H., & Vanderhart, D. L. (1984). Native cellulose: a composite of two distinct crystalline forms. *Science*, *223*, 283–285.

Blumenkrantz, N., & Asboe-Hansen, G. (1973). New method for quantitative determination of uronic acid. *Analytical Biochemistry*, *54*, 484–489.

Capek, P., Toman, R., Kardosova, A., & Rosik, J. (1983). Polysaccharides from the roots of the marshmallow (*Althaea officinalis L.*): structure of an arabinan. *Carbohydrate Research*, *117*, 133–140.

Colquhoun, I. J., de Ruiter, G. A., Schols, H. A., & Voragen, A. G. J. (1990). Identification ny NMR spectroscopy of oligosaccharides obtained by treatment of the hairy regions of apple pectin with rhamnogalacturonase. *Carbohydrate Research*, *206*, 131–144.

Cousins, S. K., & Brown, R. M. (1995). Cellulose I microfibril assembly: computational molecular mechanics energy analysis favours bonding by van der Waals forces as the initial step in crystallization. *Polymer*, *36*, 3885–3888.

Dolmetsch, H., & Dolmetsch, H. (1968). Uber die Beziehungen zwischen Kristalliten, Elementarfibrillen und zugänglichen Bereichen in Cellulose-fasern insbesondere in Holzfaserzellwänden. *Das Papier*, *22*, 1–11.

Fenwick, K. M., Jarvis, M. C., Apperley, D. C., Seymour, G. B., & Bird, C. R. (1996). Polymer mobility in cell walls of transgenic tomatoes with reduced polygalacturonase activity. *Phytochemistry*, *42*, 301–307.

Foster, T. J., Ablett, S., McCann, M. C., & Gidley, M. J. (1996). Mobility-resolved ^{13}C-NMR spectroscopy of primary plant cell walls. *Biopolymers*, *39*, 51–66.

Gardner, K. H., & Blackwell, J. (1974). The hydrogen bonding in native cellulose. *Biochim Biophysical Acta*, *343*, 232–237.

Ha, M. -A., Evans, B. W., Jarvis, M. C., Apperly, D. C., & Kenwright, A. M. (1996). CP-MAS NMR of highly mobile hydrated biopolymers: polysaccharides of *Allium* cell walls. *Carbohydrate Research*, *288*, 15–23.

Hayashi, T., Marsden, M. P. F., & Delmer, D. P. (1987). Pea xyloglucan and cellulose. Xyloglucan–cellulose interactions in vitro and in vivo. *Plant Physiology*, *83*, 384–389.

Horii, F., Hirai, A., & Kitamaru, R. (1984). Cross-polarisation/magic angle spinning ^{13}C-NMR study. Molecular chain conformations of native and regenerated cellulose. In J. C. Arthur, *Polymers for fibers and elastimers* (pp. 27–42). Washington DC: American Chemical Society.

Irwin, P. L., Gerasimowicz, W. V., Pfeffer, P. E., & Fishman, M. (1985). $^{1}H-^{13}C$ polarisation transfer studies of uronic acid polymer systems. *Journal of Agriculture and Food Chemistry*, *33*, 1197–1201.

Irwin, P. L., Pfeffer, P. E., Gerasimowicz, W. V., Pressey, R., & Sams, C. E. (1984). Ripening related perturbations in apple cell wall nuclear spin dynamics. *Phytochemistry*, *23*, 2239–2242.

Irwin, P. L., Sevilla, M. D., Chamulitrat, W., Hoffman, A. E., & Klein, J. (1992). Localized, internal, and supramolecular polyuronide motions in cell wall matrices: a comparison of solid state NMR and EPR relaxation behaviour. *Journal Agriculture and Food chemistry*, *40*, 2045–2051.

Jarvis, M. C. (1990). Solid state ^{13}C-NMR spectra of *Vigna* primary cell walls and their polysaccharide components. *Carbohydrate Research*, *201*, 327–333.

Jarvis, M. C., & Apperley, D. C. (1990). Direct observation of cell wall structure in living plant tissues by solid-state ^{13}C NMR spectroscopy. *Plant Physiology*, *92*, 61–65.

John, M. A., & Dey, P. M. (1986). Postharvest changes in fruit cell walls. *Advances in Food Research*, *30*, 139–193.

Levy, S., York, W. S., Stuike-Prill, R., Meyer, B., & Staehlin, L. A. (1991). Simulations of the static and dynamic molecular conformations of xyloglucan. The role of the fucosylated sidechain in surface-specific sidechain folding. *The Plant Journal*, *1*, 195–215.

Mitikka, M., Teeaar, R., Tenkanen, M., Laine, J., & Vuorinen, T. (1995). *Sorption of xylans on cellulose fibers*, *Proceedings of the eighth International Symposium Wood pulping chemistry* Helsinki.

Newman, R. H. (1992). ^{13}C NMR spectroscopy of multiphase biomaterials. In W. G. Glasser & H. Hatakeyma, *Viscoelasticity of BiomaterialsACS Symposium series 489* (pp. 311–319). Washington, DC: American Chemical Society.

Newman, R. H., Davies, L. M., & Harris, P. J. (1996). Solid-state ^{13}C nuclear magnetic resonance characterisation of cellulose in the cell walls of *Arabidopsis thaliana* leaves. *Plant Physiology*, *111*, 475–485.

Newman, R. H., Ha, M. -A., & Melton, L. D. (1994). ^{13}C NMR investigation of molecular ordering in the cellulose of apple cell walls. *Journal of Agriculture and Food Chemistry*, *42*, 1402–1406.

Newman, R. H., & Hemmingson, J. A. (1990). Determination of the degree of cellulose crystallinity in wood by carbon-13 nuclear magnetic resonance spectroscopy. *Holzforschung*, *44*, 351–355.

Newman, R. H., & Hemmingson, J. A. (1995). Carbon-13 NMR distinction between categories of molecular order and disorder in cellulose. *Cellulose*, *2*, 95–110.

Newman, R. H., Hemmingson, J. A., & Suckling, I. D. (1993). Carbon-13 nuclear magnetic resonance studies of kraft pulping. *Holzforschung*, *47*, 234–238.

Redgwell, R. J., MacRae, E., Hallett, I., Fischer, M., Perry, J., & Harker, R. (1997). In-vivo and in-vitro swelling of cell walls during fruit ripening. *Planta*, *203*, 162–173.

Redgwell, R. J., Melton, L. D., & Brasch, D. J. (1988). Cell-wall polysaccharides of kiwifruit (*Actinidia deliciosa*): chemical features in different tissue zones of the fruit at harvest. *Carbohydrate Research*, *182*, 241–258.

Redgwell, R. J., Melton, L. D., & Brasch, D. J. (1992). Cell wall dissolution in ripening kiwifruit (*Actinidia deliciosa*). Solubilisation of the pectic polymers. *Plant Physiology*, *98*, 71–81.

Rowland, S. O., & Howley, P. S. (1988). Structure in amorphous regions, accessible segments of fibrils, of the cotton fiber. *Textile Research Journal*, *58*, 96–101.

VanderHart, D. L., & Atalla, R. H. (1984). Studies of microstructure in native celluloses using solid-state ^{13}C NMR. *Macromolecules*, *17*, 1465–1472.

Whitney, S. E. C., Brigham, J. E., Darke, A. H., Reid, J. S. G., & Gidley, M. J. (1995). In vitro assembly of xyloglucan/cellulose networks: ultrastructural and molecular aspects. *The Plant Journal*, *8*, 491–504.

York, W. S., Harvey, L. K., Guillen, R., Albersheim, P., & Darvill, A. G. (1993). Structural analysis of tamarind seed xyloglucan oligosaccharides using β-galactosidase digestion and spectroscopic methods. *Carbohydrate Research*, *248*, 285–301.